Letter

Vertical transverse transport induced by hidden in-plane Berry curvature in two dimensions

Kyoung-Whan Kim,[1,*] Hogyun Jeong,[2,*] Jeongwoo Kim,[3,†] and Hosub Jin[2,‡]
[1]*Center for Spintronics, Korea Institute of Science and Technology, Seoul 02792, Korea*
[2]*Department of Physics, Ulsan National Institute of Science and Technology, Ulsan 44919, Korea*
[3]*Department of Physics, Incheon National University, Incheon 22012, Korea*

(Received 21 May 2021; revised 17 August 2021; accepted 17 August 2021; published 30 August 2021)

The discovery of Berry curvature (BC) has spurred a tremendous surge of research into various quantum phenomena such as the anomalous transport of electrons and the topological phases of matter. In two-dimensional crystalline systems, the conventional definition of the BC lacks the in-plane components and thus it cannot explain the transverse transport along the plane-normal direction. Here, we modify the BC to provide in-plane components in two dimensions, giving rise to the vertical Hall effects that describe out-of-plane transports in response to in-plane perturbations and their Onsager reciprocity. Our first-principles calculations show that a large in-plane BC can appear even in an atomic-thick $GdAg_2$ monolayer, and a hexagonal $BiAg_2$ monolayer can host a large BC dipole known to vanish in the conventional BC. The quantum transports driven by the hitherto-hidden BC will become more significant in recently emerging two-dimensional platforms, including van der Waals heterostructures.

DOI: 10.1103/PhysRevB.104.L081114

I. INTRODUCTION

The anomalous transport of electrons and the topological phases of matter originate from the quantum geometric phase of Bloch states, which is described by the Berry curvature (BC) [1–3]. In three-dimensional periodic systems, the crystal momentum $\mathbf{k}$ is a good quantum number and the reduced Hamiltonian $H(\mathbf{k})$ is acquired by the Bloch theorem. The eigenstates and the corresponding eigenvalues are denoted by $|n(\mathbf{k})\rangle$ and $E_n(\mathbf{k})$. The BC of the nth band has the conventional form of [4,5]

$$\mathbf{\Omega}_n^{\mathrm{3D}}(\mathbf{k}) = i \sum_{m \neq n} \frac{\langle n|\nabla_{\mathbf{k}} H|m\rangle \times \langle m|\nabla_{\mathbf{k}} H|n\rangle}{(E_n - E_m)^2}. \tag{1}$$

Hereafter, unless specified, we express $|n(\mathbf{k})\rangle$ and $E_n(\mathbf{k})$ by $|n\rangle$ and E_n for simplicity. A nonvanishing BC appears in symmetry-broken environments [5]. For a system with broken time-reversal symmetry, the integration of $\mathbf{\Omega}(\mathbf{k})$ over the momentum space links to an intrinsic anomalous Hall effect [3,6]; for a noncentrosymmetric system, the integration of $\partial_{k_i}\mathbf{\Omega}(\mathbf{k})$, referred to as the BC dipole, gives rise to the quantum nonlinear Hall effect [7–9] and the photogalvanic effect [10–13].

By contrast, for two-dimensional systems located in the xy plane, k_z is not a good quantum number and only the z component of the BC is defined by Eq. (1). Through the dimensional crossover from three to two dimensions (Fig. 1), one can gain insight into the incompleteness of the existing definition of the BC. The left panels of Fig. 1 show three-dimensional materials with broken time-reversal symmetry and broken inversion symmetry, respectively. When a ferromagnetic moment is present along the x direction, the net flux of the x-component BC induces an anomalous Hall effect. As illustrated in Fig. 1(a), for example, an electric field along the z direction (E_z) generates an electrical current along the y direction (J_y) [3]. Similarly, when electric polarization is present along the z direction, a helical structure of BC around the polarization ($\mathbf{\Omega} \sim \hat{\mathbf{z}} \times \mathbf{k}$) carries a nonzero BC dipole, leading to a nonlinear Hall current (J_z) in response to an oscillating electric field ($E_{\omega,x}$), as shown in Fig. 1(b) [11,14]. All of these transverse transport phenomena are engendered by the well-defined x, y components of the BC in three dimensions. We now reduce to the lower dimension by gradually decreasing the thickness of the system (Fig. 1, right panels). Because the symmetry breaking remains the same, one can speculate that the aforementioned anomalous responses would be retained during the dimensional reduction. In a recent experiment [15], the giant vertical nonlinear Hall effect has been reported upon varying the thickness of WTe_2 and $MoTe_2$ films. The conventional BC in two dimensions, however, cannot describe these responses because Eq. (1) does not include the in-plane components. Therefore, it is necessary to generalize the BC formula to provide all three components for a complete description and applications of anomalous transport in two dimensions.

In this paper, we generalize the BC in two dimensions and predict the generation of a large vertical Hall current in response to an in-plane electric field. The reformulated BC has in-plane components that are absent in the conventional BC. Using perturbation theory, we derive that the in-plane BC governs the vertical transverse transports illustrated in the right panels of Fig. 1. Our density functional theory (DFT)

*These authors contributed equally to this work.
†Corresponding author: kjwlou@inu.ac.kr
‡Corresponding author: hsjin@unist.ac.kr

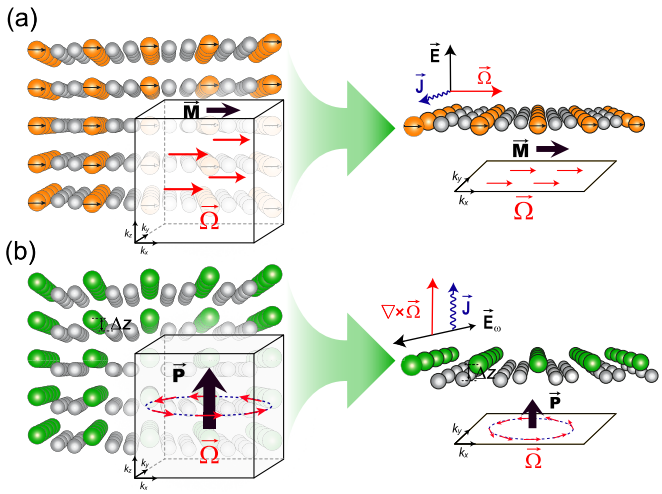

FIG. 1. (a) Left: The BC flux is induced by broken time-reversal symmetry in a three-dimensional solid. Right: In dimensional crossover preserving the symmetry breaking, in-plane BC appears with the corresponding linear anomalous Hall effect in two dimensions. (b) Left: The helical BC texture emerges from broken inversion symmetry in a three-dimensional solid. Right: During dimensional reduction, the helical texture of in-plane BC is preserved, resulting in the out-of-plane BC dipole and the corresponding nonlinear anomalous Hall effect in two dimensions.

calculations reveal that the in-plane BC can dominate over the conventional out-of-plane component even in the extreme limit of atomic-thick two-dimensional systems in which the vertical motion is suppressed. We consider two representative examples of inversion-broken and time-reversal-broken systems: $BiAg_2$ and $GdAg_2$ monolayers. Against the general belief that the BC dipole vanishes in two-dimensional hexagonal systems [7], a large dipole component of BC survives in a $BiAg_2$ monolayer based on our formalism. We also performed the time-dependent DFT calculations, explicitly demonstrating the vertical Hall currents induced by the in-plane BC.

II. GENERALIZATION OF BC IN TWO DIMENSIONS

We present the following generalization of the BC by applying a position operator formalism [16–18]. In a periodic system, the physical meaning of $\nabla_{\mathbf{k}}H$ in Eq. (1) is the velocity operator multiplied by $\hbar$. Therefore, $\langle n|\partial_{k_z}H|m\rangle$ can be replaced with $\langle n|i[H,z]|m\rangle = i(E_n - E_m)\langle n|z|m\rangle$ for $n \neq m$ in a system confined along the z direction. Notably, $\langle n|z|m\rangle$ is well defined in a finite system, enabling the in-plane BC components to be reformulated. The modified version of Eq. (1) for two-dimensional systems is then

$$\mathbf{\Omega}_n^{\mathrm{2D}}(\mathbf{k}) = i\sum_{m\neq n}\frac{\langle n|\nabla_{\mathbf{k}}H|m\rangle \times \langle m|\nabla_{\mathbf{k}}H|n\rangle}{(E_n - E_m)^2} + 2\mathrm{Re}\sum_{m\neq n}\frac{\langle n|\nabla_{\mathbf{k}}H|m\rangle \times \langle m|z\hat{\mathbf{z}}|n\rangle}{E_n - E_m}. \quad (2)$$

The first term is the conventional out-of-plane component, and the second term gives in-plane BC, which has not yet been considered. Unlike $\mathbf{\Omega}^{\mathrm{3D}}$ in Eq. (1), the two-dimensional $H(\mathbf{k})$ is not sufficient to express $\mathbf{\Omega}^{\mathrm{2D}}$, requiring additional information about the *hidden* degree of freedom along the z direction. Note that the second term in Eq. (2) is not strictly a *curvature* in the conventional sense, which originates from the holonomy of the electronic states in $\mathbf{k}$ space. But in this paper we call it a generalized version of a curvature because it becomes equivalent to the conventional curvature when the periodicity along the z direction is restored. We also note that similar generalizations are possible for one and zero dimensions [19]. We hereafter omit the superscript "2D" unless specified.

The reformulated BC indeed describes the anomalous responses illustrated in the right panels in Fig. 1. In the presence of a constant electric field (E) along the z direction, the perturbed eigenstate is written as $|\widetilde{n}\rangle = |n\rangle - \sum_{m\neq n}|m\rangle\langle m|eEz|n\rangle/(E_n - E_m)$ in the length gauge. The transverse in-plane current is then given by the in-plane components of the reformulated BC:

$$\mathbf{J} = -\frac{e}{\hbar}\sum_{\mathbf{k},n} f_{\mathbf{k}}\langle\widetilde{n}|\nabla_{\mathbf{k}}H|\widetilde{n}\rangle = \frac{e^2}{\hbar}E\hat{\mathbf{z}}\times\sum_{\mathbf{k},n} f_{\mathbf{k}}\mathbf{\Omega}_n(\mathbf{k}), \quad (3)$$

where $f_{\mathbf{k}}$ is the electron distribution function. In two dimensions, Eqs. (2) and (3) account for a type of anomalous Hall transport in response to a vertical electric field [Fig. 1(a), right panel]. Also, the Onsager reciprocity indicates that an in-plane electric field can induce the z-directional shift of an electron so that a charge current is pumped into an adjacent metal electrode stacked in the vertical direction. In the absence of the inversion symmetry, a semiclassical theory [7] shows that the nonequilibrium distribution function perturbed by an external electric field, $\delta f_{\mathbf{k}} \propto \mathbf{E}\cdot\nabla_{\mathbf{k}}f_{\mathbf{k}}$, may generate the nonlinear Hall and photogalvanic currents [Fig. 1(b), right panel], the magnitudes of which are both proportional to the BC dipole.

III. HELICAL IN-PLANE BC IN A POLAR $BiAg_2$ MONOLAYER

Here we investigate the generalized BC in an atomic-thick $BiAg_2$ monolayer, in which the out-of-plane polar displacement (Δz) of Bi atoms [Fig. 2(a)] [20] induces substantial in-plane BC and its dipole. Figure 2(b) is the electronic band structure calculated from the first-principles calculations [19] and shows a Rashba-like spin splitting induced by the inversion asymmetry. As illustrated in Fig. 1(b), the polar displacement is expected to display a helical structure of the in-plane BC and the corresponding out-of-plane BC dipole. In Fig. 2(c), a clockwise helical BC vector is drawn in the momentum space with the chemical potential μ set to 0.55 eV (green horizontal lines). Figure 2(d) shows the out-of-plane BC dipole density, $d_z(\mathbf{k}) = (1/2)[\nabla_{\mathbf{k}}\times\mathbf{\Omega}(\mathbf{k})]_z$, arising from the helical in-plane BC, the maximum size of which reaches 500 Å^3. By integrating the BC dipole density over the first Brillouin zone, we plot the BC dipole as a function of μ in Fig. 2(e). According to Fig. 2(f), the helical in-plane BC is a direct consequence of the polar displacement.

The resulting BC dipole implies the significance of our generalized formalism. According to the conventional BC

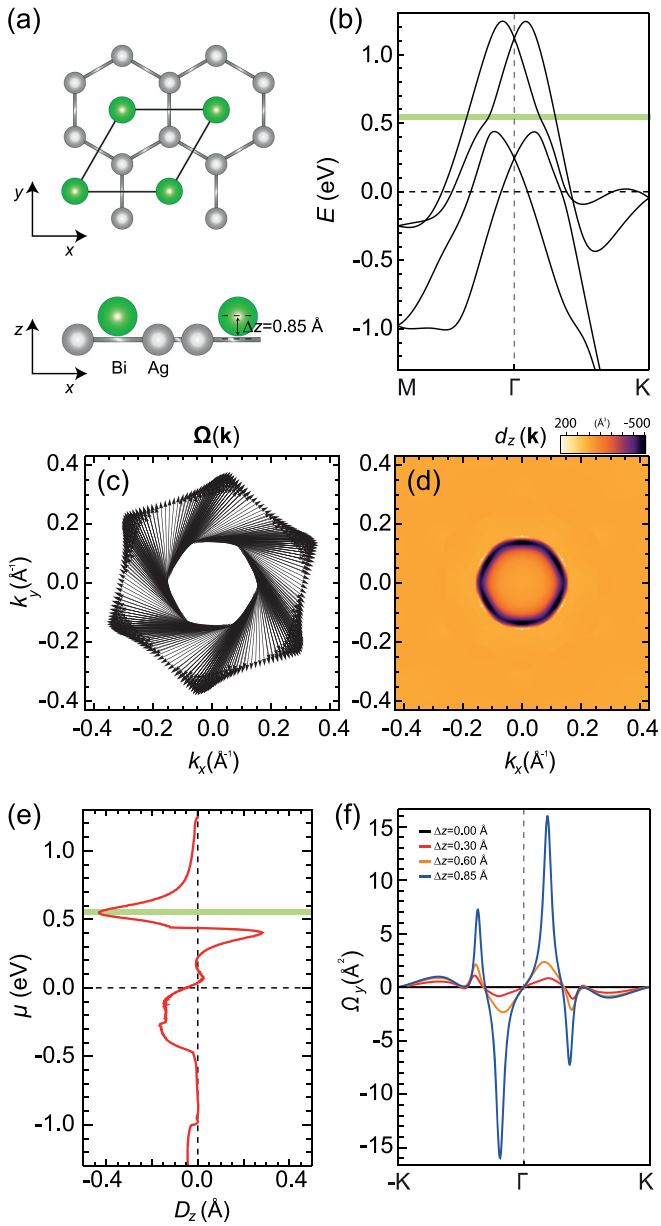

FIG. 2. (a) Atomic structure of the $BiAg_2$ monolayer. The polar displacement of the Bi atoms breaks the inversion symmetry. (b) The electronic structure of the $BiAg_2$ monolayer. (c) The in-plane BC vectors in the momentum space, as calculated at the chemical potential $\mu = 0.55$ eV. (d) The BC dipole density (d_z) in the momentum space calculated from the curl of the BC vectors in (c). (e) Plot of the BC dipole (D_z) (the integration of d_z over the first Brillouin zone) as a function of the chemical potential. (f) Ω_y calculated along the k_x direction for $k_y = 0$ by varying the polar displacement. The result indicates that the in-plane BC is proportional to the amount of symmetry breaking induced by the polar displacement.

formula, the BC dipole vanishes in two-dimensional crystals belonging to the C_{3v} symmetry class [7], and hence it has been widely believed that the nonlinear Hall effect is absent in two-dimensional hexagonal crystals. On the contrary, our calculations exhibit a *hidden* BC dipole in a $BiAg_2$ monolayer, which is also in the C_{3v} symmetry class. Furthermore, the maximum size of the BC dipole density is more than two orders of magnitude larger than that arising from the conventional out-of-plane BC in III-V semiconductor [110] quantum wells (≈ 1 Å^3) [12]. The resultant BC dipole is as large as -0.4 Å, which is comparable [19] to the enormously enhanced value at the topological phase transition in BiTeI [14]. It is also comparable to the large BC dipole (induced by the out-of-plane BC) of WTe_2 multilayers [8,9,13] and SnTe monolayers [21].

To investigate the microscopic mechanism of the in-plane BC in a $BiAg_2$ monolayer, we constructed a four-band model based on p orbitals in Bi atoms and s orbitals in Ag atoms. As mentioned above [after Eq. (2)], unlike the conventional BC, the in-plane BC cannot be calculated only by the Hamiltonian and its eigenstates, but additional information on matrix elements of the out-of-plane position operator z is necessary. By carefully taking them into account, we derive [19]

$$\mathbf{\Omega}_{\rm in}^{p_z} \propto \Delta z \hat{\mathbf{z}} \times \mathbf{k}, \tag{4}$$

up to first order in sp hybridization and the polar displacement. Here $\mathbf{\Omega}_{\rm in}^{p_z}$ is the in-plane BC for the p_z band and Δz is the polar displacement of Bi atoms [Fig. 2(a)]. The in-plane BC forms a helical BC structure induced by the inversion breaking polar displacement as we depict in Fig. 1(b). The out-of-plane BC dipole density from the helical BC texture is then given by $\frac{1}{2}\nabla_{\mathbf{k}} \times \mathbf{\Omega}_{\rm in}^{p_z} \propto \Delta z \hat{\mathbf{z}}$. The in-plane BCs for the other bands show similar behaviors, as implied by the symmetry. Recalling that the matrix elements of the position operator z are essential for our calculation, the finite spatial extension of electron clouds along the surface normal direction and interorbital mixing triggered by the polar displacement play a crucial role in providing the in-plane BC.

IV. IN-PLANE BC FLUX IN A FERROMAGNETIC $GdAg_2$ MONOLAYER

Now we consider the second system, a $GdAg_2$ monolayer, where the in-plane ferromagnetic moments of Gd atoms break the time-reversal symmetry [22,23]. The electronic band structure corresponding to the Gd moments aligned along the x direction [Fig. 3(a)] is shown in Fig. 3(b). As illustrated in Fig. 1(a), the in-plane ferromagnetic moment yields the yz component of the anomalous Hall conductivity (σ_{yz}) given by the integration of the x component BC (Ω_x) multiplied by e^2/h [Eq. (3)]. The calculated σ_{yz} reaches 0.62 e^2/h in the vicinity of the Fermi level [Fig. 3(c)], which is comparable to the quantized Hall conductivity of Chern insulators [24,25]. The substantial size of σ_{yz} in the $GdAg_2$ monolayer implies that, even in atomically thin films, the vertical Hall response cannot be neglected. The unveiled σ_{yz} can provide a proper interpretation of some measurement schemes the microscopic formulations of which in two dimensions remain elusive, such as the longitudinal magneto-optic Kerr effect of in-plane two-dimensional ferromagnets [26,27].

Figures 3(d)–3(f) show maps of the three components of the BC when the chemical potential is tuned slightly above the Fermi level [yellow line in Fig. 3(b)]. In Fig. 3(d), the maximum magnitude of Ω_x (283 Å^2) emerges along the Γ-K line from the anticrossing between $m_z = \pm 1$ and ± 2 bands

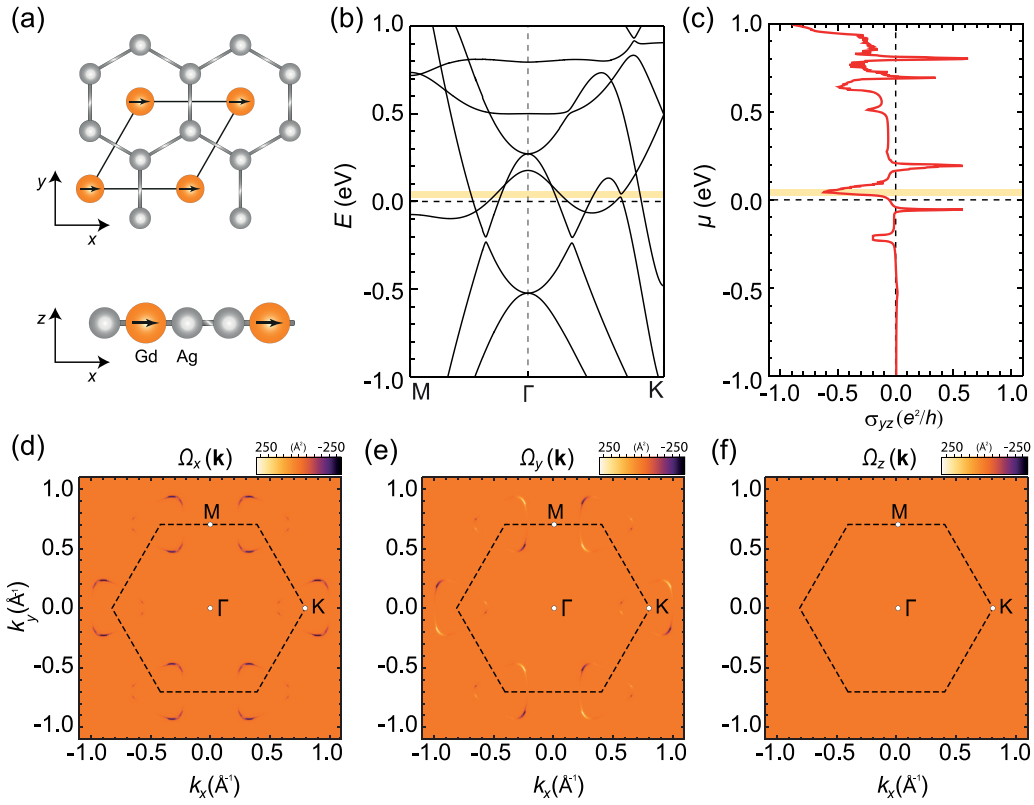

FIG. 3. (a) Atomic structure of the $GdAg_2$ monolayer. The in-plane ferromagnetic moment of the Gd atoms breaks the time-reversal symmetry. (b) The electronic structure of the $GdAg_2$ monolayer. (c) The yz component of the anomalous Hall conductivity (the integration of Ω_x over the first Brillouin zone) as a function of the chemical potential (μ). (d)–(f) Maps of each component of $\boldsymbol{\Omega}$ calculated at the chemical potential depicted as yellow lines in (b) and (c). The results are consistent with the yz mirror reflection and inversion symmetry of the system. Whereas Ω_x is large, the other components are negligible (Ω_z) or vanish when integrated out (Ω_y).

composed of d_{yz}/d_{zx} and $d_{xy}/d_{x^2-y^2}$ orbitals, respectively. The integration of Ω_y vanishes because of the yz mirror plane perpendicular to the ferromagnetic moment [Fig. 3(e)], and Ω_z in Fig. 3(f) is negligible ($\lesssim 1$ Å^2).

In Supplemental Material [19], we construct a model Hamiltonian and the matrix element of the position operator z. We calculate the in-plane BC for one of the $m_z = \pm 2$ bands as

$$\boldsymbol{\Omega}_{\text{in}} \propto \alpha k_x \mathbf{k}, \tag{5}$$

up to first order in spin-orbit coupling parameter α and the inverse of the band splitting energy. Note that $\Omega_x \propto k_x^2$ can give a nonvanishing BC monopole, while $\Omega_y \propto k_x k_y$ cannot. And the in-plane BC distribution of $\Omega_x \propto k_x^2$ and $\Omega_y \propto k_x k_y$ is also consistent with C_{2x} rotation and M_x mirror reflection symmetry of the system. These features are consistent with Figs. 3(d) and 3(e). Our analytic theory reveals that, under the in-plane spin polarization, spin-orbit coupling acts as a ladder operator to raise or lower the orbital angular momentum, which intertwines the lateral and vertical movements of electrons and consequently gives rise to the large Ω_x.

V. TIME-DEPENDENT DFT CALCULATIONS FOR THE VERTICAL HALL EFFECT

By performing time-dependent DFT calculations [19] for a $GdAg_2$ monolayer, we explicitly demonstrate the anomalous Hall current induced by the in-plane BC shown in Fig. 3(c). Figure 4(a) shows the time-varying electric field obtained by the Fourier transform of the frequency spectrum shown in the inset. By applying the electric field along the y direction (E_y), we obtain the transverse current along the z direction (J_z), which is perpendicular to both the electric field ($\mathbf{E}$) and the magnetic moment ($\mathbf{M}$) [red curve in Fig. 4(b)]. We also observe an oscillatory current profile the period of which approximately coincides with that of the electric field. Because of the lack of an additional relaxation process in our simulation, the oscillating current persists even after $t = 2.0$ fs when the external field is negligible. The blue curve in Fig. 4(b) shows the Hall current along the y direction (J_y) under an electric field along the z direction. J_z and J_y are of the same magnitude but with opposite signs, clearly showing the expected Onsager reciprocity $\sigma_{yz} = -\sigma_{zy}$.

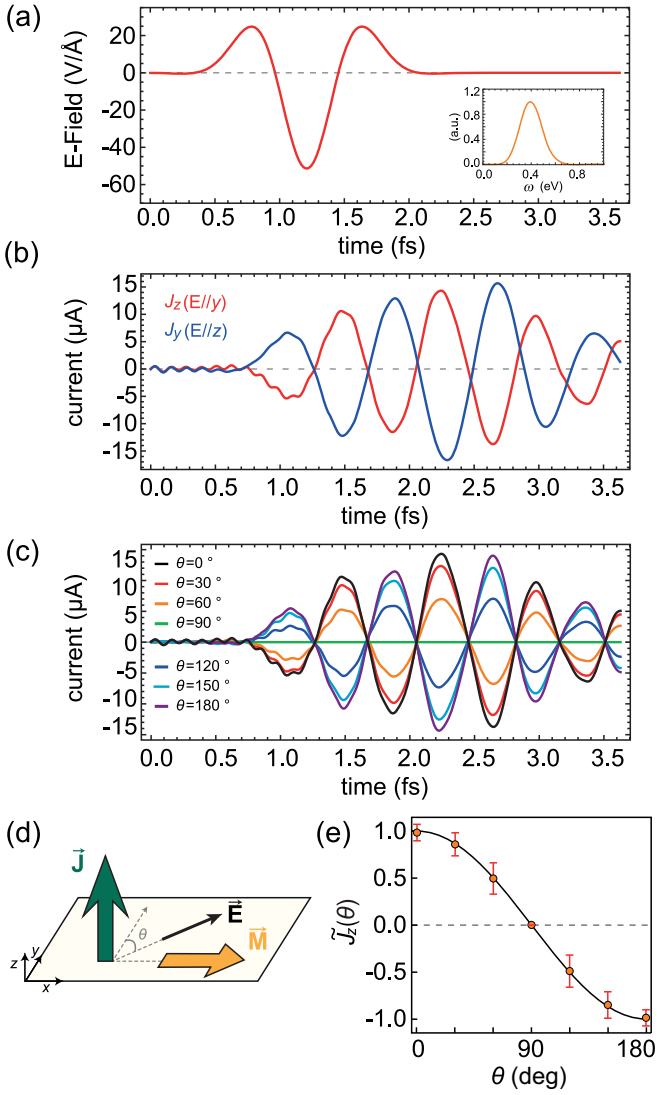

FIG. 4. (a) The applied electric field to the $GdAg_2$ monolayer as a function of time in the time-dependent DFT calculations. Inset: Frequency spectrum of the applied electric field. (b) Time-varying current along the y direction (J_y) under the electric field along the z direction (red) and that along the z direction (J_z) under the electric field along the y direction (blue). (c) The J_z calculated by rotating the in-plane directions (θ) of the applied electric field. (d) Schematic of the geometry of the simulation. (e) Time-averaged normalized currents as a function of θ. The error bars are determined by the standard deviation over the evaluation times. The solid black line denotes $\cos\theta$.

In addition, we investigated the out-of-plane current response by varying the direction of the applied electric field within the plane [Fig. 4(c)]. Here, θ is the angle of the electric field that deviates from the y direction [Fig. 4(d)]. The magnitude of J_z is maximum when the electric field is perpendicular to the direction of the ferromagnetic moment (black and purple curves), whereas it completely vanishes when the electric field is parallel to **M** (green curve). Figure 4(e) shows a plot of the normalized Hall current as a function of θ [19]. Despite the complicated oscillating feature of J_z in time, all data fall along a single cosine curve, confirming that $\mathbf{J}_H \sim \mathbf{E} \times \mathbf{\Omega}$. Therefore, the transverse current J_z is directly determined by the anomalous Hall conductivity σ_{zy} in Eq. (3) and it thus is the manifestation of the in-plane BC. The transverse transport phenomena in our simulation indeed represent an anomalous Hall effect in a two-dimensional in-plane ferromagnet the response function of which is governed by the in-plane BC.

VI. CONCLUSION

We generalize the BC in two dimensions, unravelling, in particular, the existence of the in-plane components and corresponding responses. The in-plane components capture linear and nonlinear anomalous Hall effects along the surface normal direction, which cannot be described by the conventional BC formalism. The vertical responses originate from the spatial distribution of electrons along the confined direction and are inevitable in real two-dimensional systems. The giant in-plane BC appearing in the atomic-thick limit represents an advancement beyond proof of concept and provides a perspective into quantum transport in low dimensions. Furthermore, in the currently prevailing van der Waals heterostructures [28–31], the generalized BC can be tailored through adjustment of the symmetry in diverse ways, enriching the scope and functionality of two-dimensional systems.

ACKNOWLEDGMENTS

K.-W.K. was supported by the KIST Institutional Program under Grant No. 2E31032 and the National Research Foundation of Korea (NRF) under Grants No. 2020R1C1C1012664 and No. 2019M3F3A1A02071509. J.K. was supported by an NRF grant funded by the Korea government (MSIT) under Grant No. 2020R1F1A1048143. H. J. and H. J. were supported by the NRF under Grants No. 2021M3H4A1A03054864, No. 2019R1A2C1010498, and No. 2017M3D1A1040833.

[1] D. J. Thouless, M. Kohmoto, M. P. Nightingale, and M. den Nijs, Phys. Rev. Lett. **49**, 405 (1982).
[2] M. V. Berry, Proc. R. Soc. A **392**, 45 (1984).
[3] N. Nagaosa, J. Sinova, S. Onoda, A. H. MacDonald, and N. P. Ong, Rev. Mod. Phys. **82**, 1539 (2010).
[4] Y. Yao, L. Kleinman, A. H. MacDonald, J. Sinova, T. Jungwirth, D.-s. Wang, E. Wang, and Q. Niu, Phys. Rev. Lett. **92**, 037204 (2004).
[5] D. Xiao, M.-C. Chang, and Q. Niu, Rev. Mod. Phys. **82**, 1959 (2010).
[6] Z. Fang, N. Nagaosa, K. S. Takahashi, A. Asamitsu, R. Mathieu, T. Ogasawara, H. Yamada, M. Kawasaki, Y. Tokura, and K. Terakura, Science **302**, 92 (2003).
[7] I. Sodemann and L. Fu, Phys. Rev. Lett. **115**, 216806 (2015).
[8] Q. Ma, S.-Y. Xu, H. Shen, D. MacNeill, V. Fatemi, T.-R. Chang, A. M. Mier Valdivia, S. Wu, Z. Du, C.-H. Hsu *et al.*, Nature (London) **565**, 337 (2019).

[9] K. Kang, T. Li, E. Sohn, J. Shan, and K. F. Mak, Nat. Mater. **18**, 324 (2019).
[10] J. E. Sipe and A. I. Shkrebtii, Phys. Rev. B **61**, 5337 (2000).
[11] E. Deyo, L. E. Golub, E. L. Ivchenko, and B. Spivak, arXiv:0904.1917 (2009).
[12] J. E. Moore and J. Orenstein, Phys. Rev. Lett. **105**, 026805 (2010).
[13] S.-Y. Xu, Q. Ma, H. Shen, V. Fatemi, S. Wu, T.-R. Chang, G. Chang, A. M. M. Valdivia, C.-K. Chan, Q. D. Gibson *et al.*, Nat. Phys. **14**, 900 (2018).
[14] J. I. Facio, D. Efremov, K. Koepernik, J.-S. You, I. Sodemann, and J. van den Brink, Phys. Rev. Lett. **121**, 246403 (2018).
[15] A. Tiwari, F. Chen, S. Zhong, E. Drueke, J. Koo, A. Kaczmarek, C. Xiao, J. Gao, X. Luo, Q. Niu *et al.*, Nat. Commun. **12**, 2049 (2021).
[16] J. Bellissard, A. v. Elst, and H. S. Baldes, J. Math. Phys. **35**, 5373 (1994).
[17] E. Drigo and R. Resta, Phys. Rev. B **101**, 165120 (2020).
[18] D. Hara, M. S. Bahramy, and S. Murakami, Phys. Rev. B **102**, 184404 (2020).
[19] See Supplemental Material at http://link.aps.org/supplemental/10.1103/PhysRevB.104.L081114 for Refs. [32–39], for numerical details and derivations of Eqs. (4) and (5).
[20] C. R. Ast, J. Henk, A. Ernst, L. Moreschini, M. C. Falub, D. Pacilé, P. Bruno, K. Kern, and M. Grioni, Phys. Rev. Lett. **98**, 186807 (2007).
[21] J. Kim, K.-W. Kim, D. Shin, S.-H. Lee, J. Sinova, N. Park, and H. Jin, Nat. Commun. **10**, 3965 (2019).
[22] M. Ormaza, L. Fernández, M. Ilyn, A. Magaña, B. Xu, M. J. Verstraete, M. Gastaldo, M. A. Valbuena, P. Gargiani, A. Mugarza *et al.*, Nano Lett. **16**, 4230 (2016).
[23] B. Feng, R.-W. Zhang, Y. Feng, B. Fu, S. Wu, K. Miyamoto, S. He, L. Chen, K. Wu, K. Shimada *et al.*, Phys. Rev. Lett. **123**, 116401 (2019).
[24] F. D. M. Haldane, Phys. Rev. Lett. **61**, 2015 (1988).
[25] C.-Z. Chang, J. Zhang, X. Feng, J. Shen, Z. Zhang, M. Guo, K. Li, Y. Ou, P. Wei, L.-L. Wang *et al.*, Science **340**, 167 (2013).
[26] K. F. Mak, J. Shan, and D. C. Ralph, Nat. Rev. Phys. **1**, 646 (2019).
[27] T. Lan, B. Ding, and B. Liu, Nano Select **1**, 298 (2020).
[28] A. K. Geim and I. V. Grigorieva, Nature (London) **499**, 419 (2013).
[29] K. S. Novoselov, A. Mishchenko, A. Carvalho, and A. H. Castro Neto, Science **353**, aac9439 (2016).
[30] Y. Cao, V. Fatemi, A. Demir, S. Fang, S. L. Tomarken, J. Y. Luo, J. D. Sanchez-Yamagishi, K. Watanabe, T. Taniguchi, E. Kaxiras *et al.*, Nature (London) **556**, 80 (2018).
[31] J. Liu, Z. Ma, J. Gao, and X. Dai, Phys. Rev. X **9**, 031021 (2019).
[32] K. Dewhurst, S. Sharma, L. Nordström, F. Cricchio, O. Grånäs, H. Gross, C. Ambrosch-Draxl, C. Persson, F. Bultmark, C. Brouder *et al.*, the Elk code, https://elk.sourceforge.net.
[33] J. P. Perdew, K. Burke, and M. Ernzerhof, Phys. Rev. Lett. **77**, 3865 (1996).
[34] V. I. Anisimov, F. Aryasetiawan, and A. I. Lichtenstein, J. Phys.: Condes. Matter **9**, 767 (1997).
[35] J.-S. You, S. Fang, S.-Y. Xu, E. Kaxiras, and T. Low, Phys. Rev. B **98**, 121109(R) (2018).
[36] Y. Zhang, Y. Sun, and B. Yan, Phys. Rev. B **97**, 041101(R) (2018).
[37] Y. Zhang, J. van den Brink, C. Felser, and B. Yan, 2D Mater. **5**, 044001 (2018).
[38] H. Wang and X. Qian, Sci. Adv. **5**, eaav9743 (2019).
[39] J. K. Dewhurst, K. Krieger, S. Sharma, and E. K. U. Gross, Comput. Phys. Comm. **209**, 92 (2016).